Vol. 3, No. 1 January 1993

GSA TODAY

A Publication of the Geological Society of America

INSIDE

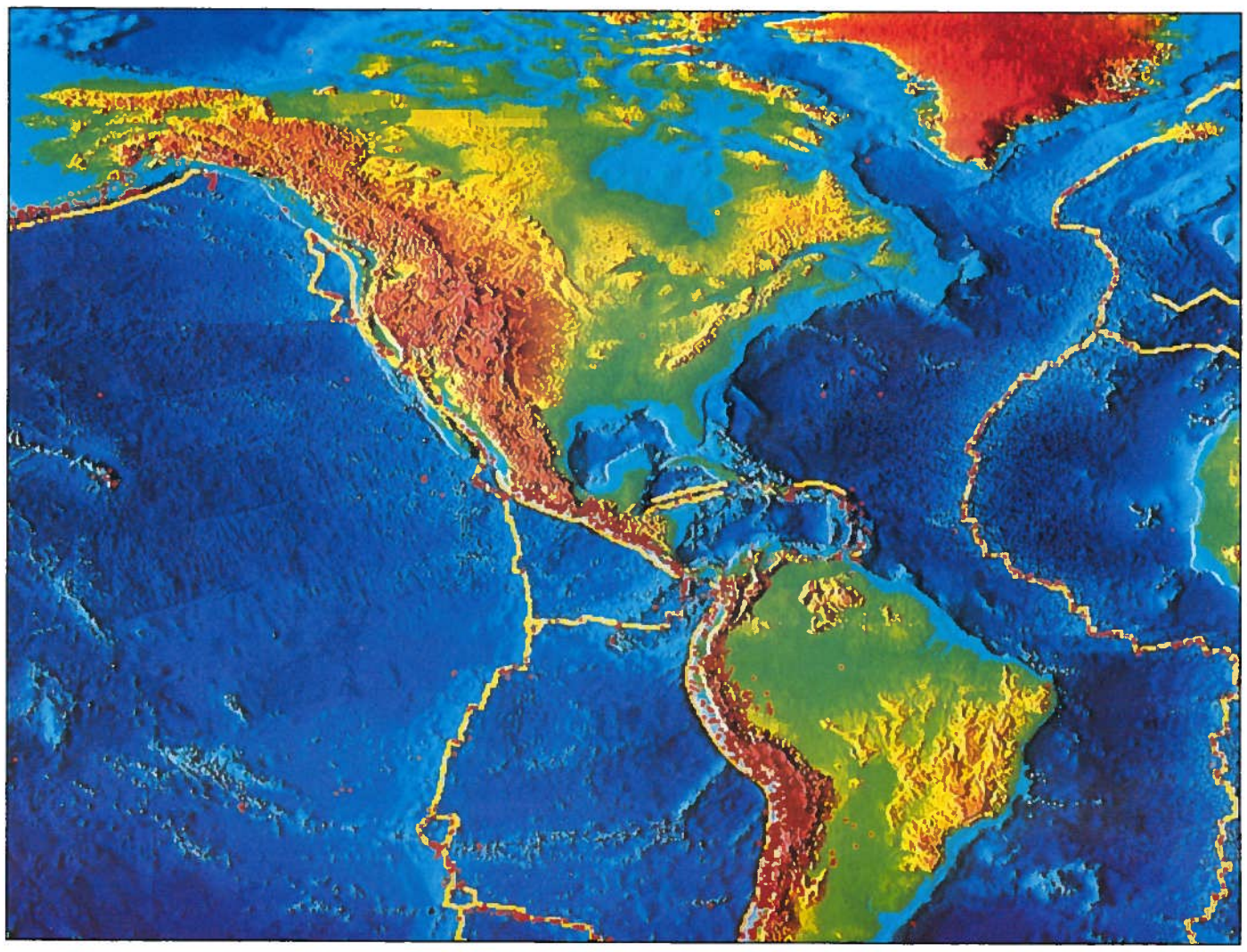

Figure 1. Color shaded relief images of the East Pacific Rise and the Mid-Atlantic Ridge .

It's Only Topography: Part 1

Ken C. Macdonald, Daniel S. Scheirer, Suzanne Carbotte
Department of Geological Sciences and Marine Sciences Institute, University of California, Santa Barbara, CA 93106

P. J. Fox
Graduate School of Oceanography, University of Rhode Island, Kingston, RI 02881

Editor's Note

The science article in this issue is the first of two parts, the second part of which will be published in February. The article summarizes much recent work on mapping the ocean floor. As Macdonald et al. point out, we have made much less progress in the past 500 years mapping the part of Earth's surface covered by the oceans than we have in the past 20 years mapping the surface of our neighboring planets. This ironic situation inspired a series in *GSA Today* on planetary surfaces which includes several previous articles as well as this one.

Because this article represents a major synthesis of a great deal of new information, and because of space limitations in *GSA Today,* we have elected to publish the paper in two parts, this month and next. We do not plan to make a habit of having articles appear in two installments, however. Accordingly, the space limitations on articles for *GSA Today* will remain as they have been.

—Eldridge M. Moores

ABSTRACT

New swath-mapping sonar systems have revealed the structure of the mid-ocean ridge and surrounding deep-ocean floor with unprecedented clarity. These images show that the ridge is partitioned into segments by a variety of offsets such as transform faults, overlapping spreading centers, and very fine scale discontinuities, which are barely detectable. The smallest scale segments are the fundamental building blocks for creation of new oceanic crust. They are only ~2–20 km long and are active, distinct units for only 100–10 000 yr. At fast-spreading centers, the axial neovolcanic zone is at a persistent 300–400 m elevation produced by the buoyancy of hot rock and magma; it is not a volcanic construction, so there is almost no vestige of it off-axis. Along most of its length, the spreading center is characterized by an axial summit caldera produced by volcanic inflation and collapse. The size and shape of the axial high are very sensitive indicators of a relatively steady and robust magma supply at fast-spreading ridges, and they have been used to predict the location of magma chambers and to forecast recent volcanic eruptions, including one witnessed from the submersible *Alvin* in March–April 1991. At intermediate spreading rates, the axial region cools sufficiently for a volcanic constructional edifice to develop episodically and for normal faulting to occur along an axial graben. Under these conditions axial volcanoes are split in two by the axial graben, and remnants can be found on the flanks of spreading centers. At slow-spreading ridges, the magma budget is relatively starved, as indicated by a persistent axial rift valley, a highly discontinuous neovolcanic zone, and strong asymmetry in profiles along and across the strike of the ridge.

INTRODUCTION

When we read a year ago about the mapping of Venus in *GSA Today* (Head and Saunders, 1991), the Magellan mission had provided spectacular images of 10%–20% of that planet's surface, and now Magellan has scanned more than 90% of the surface of Venus. In the 500 years since Ferdinand Magellan circumnavigated the world's oceans, oceanographers have scanned less than 10% of the deep ocean floor at the resolution provided by spacecraft Magellan's synthetic aperture radar images. Why has oceanography lagged so far behind the space effort? It was not until after World War II that any systematic effort was launched to map the ocean floor. To the present day, efforts to accurately map the seafloor are made from ships with sonar systems, because electromagnetic waves do not travel far through sea water. Progress has been slow, when compared to the mission to Venus, because oceanographic ships wallow over the waves at 18 km/h rather than soaring through space at 19 500 km/h. Furthermore, the U.S. oceanographic fleet is funded at levels much lower than NASA (1/50), and the acquisition and support of new mapping tools for the fleet has been a slow process. At present, four of the university-operated ships are equipped with high-resolution mapping systems, and plans are in place for the acquisition of three more systems over the next several years. However, these systems are not routinely operated because of lack of funds, and there is currently no plan to map systematically the shape of the global abyss, Earth's last frontier.

SEGMENTATION OF THE MID-OCEAN RIDGE

When viewed in an along-axis perspective, the axial depth and continuity of the mid-ocean ridge is segmented at various scales and in various ways. At the longest wavelengths, the along-strike axial profile of the ridge is characterized by a broad swell with dimensions in excess of 1000 km (Fig. 1). The crests of these swells are defined by hot spots, reach anomalously shallow levels, and are associated with excessive and long-lived magmatic budgets. At shorter wavelengths (a few tens to hundreds of kilometres), the global ridge system, independent of spreading rate or proximity to hot spots, is partitioned into discrete segments by a family of ridge-axis discontinuities that have distinctive structural signatures. Because these offsets exhibit distinctive morphologic and geochemical characteristics, in both space and time, they, and the ridge segments they partition, have been arranged in a hierarchical classification scheme of orders 1–4 (Table 1; Fig. 2) (for a review, see Schouten et al. [1985], Langmuir et al. [1986], Macdonald et al. [1988], and Macdonald and Fox [1990]).

Transform faults define first-order segments; they are large offsets of opposing ridge segments in terms of both distance (tens to hundreds of kilometres) and age (approximately one to tens of millions of years). They link ridge segments along a narrow strike-slip fault zone against which terrain parallel to the ridge axis is truncated (Figs. 3A, 4, 5A). These boundaries are stable for long periods of time (millions of years). Their aseismic extensions describe parts of small circles, and these extensions can be traced as continuous

Topography *continued on p. 24*

Topography *continued from p. 1*

lineaments for hundreds to thousands of kilometres across the flanks of the ridge. Transform-fault boundaries will be conditioned by, and will condition, accretionary processes, because the fault juxtaposes a barrier of aged lithosphere against the zero-age axis of the ridge segment (e.g., Fox and Gallo, 1984).

In contrast, ridge-axis discontinuities of the second and third order include a range of offset geometries (e.g., overlapping spreading centers along the East Pacific Rise; oblique relay zones along the Mid-Atlantic Ridge [Searle and Laughton, 1977]), and are small offsets of the opposing ridge segments in terms of both distance (less than a few tens of kilometres) and age (<~1 Ma) (Figs. 3A, 4, 5A, 5B). At second- and third-order discontinuities, structures indicative of a through-going zone of shear and rigid-plate-boundary behavior are not spatially sustained, suggesting that these offset geometries are not stable for long periods of time. These medium-order ridge-axis discontinuities are caused by differential asymmetric spreading, small changes in spreading direction, and variations in the process of melt generation (e.g., Lonsdale, 1989; Perram and Macdonald, 1990). The distinction between second- and third-order offsets is that the magnitude of a third-order offset is relatively small (less than a few kilometres), and there is little or no trace of third-order features off-axis (i.e., third-order segmentation is not long-lived, $<10^5$ yr).

The traces of second-order discontinuities are found as swaths of disturbed terrain flanking the ridge axis (called discordant zones), and generally do not trace small circles about the pole of opening (Figs. 4, 5A, 5B). Second-order segmentation patterns can follow one of at least two evolutionary paths: they migrate along-strike, leaving a V-shaped wake of abandoned ridge tips and basins; or they remain approximately in the same place, but oscillate back and forth along the ridge (Lonsdale, 1985; Macdonald et al., 1987; Wilson, 1990). It has been documented along the fast end of the accretionary spectrum (East Pacific Rise) that these discontinuities form abruptly, migrate rapidly along strike at variable velocities and directions, and are short-lived (less than a few million years) (Macdonald et al., 1988; Carbotte and Macdonald, 1992). Along-strike propagation speeds of up to 4000 mm/yr have been documented on the East Pacific Rise near lat 18°S (Cormier and Macdonald, 1991). Although less well constrained at the slow end of the accretionary spectrum (<40 mm/yr), second-order discontinuities appear to be longer lived (millions of years), propagate less rapidly, and exhibit a range of behavior in terms of spatial positioning (e.g., Sempere et al., 1990; Fox et al., 1991). They can remain fixed or they can migrate along strike, creating V-shaped patterns characterized by obliquely oriented ridges and basins. At all spreading rates, it is possible for one type of ridge-axis discontinuity to evolve into another by sustained asymmetric spreading of adjoining ridge segments (Perram and Macdonald, 1990; Grindlay et al., 1991). Characteristically, the terrain in close proximity to the discordant zones is highly magnetized, probably reflecting the eruption of highly fractionated basalts (e.g., Carbotte and Macdonald, 1992).

The different types of boundaries outlined above partition the mid-ocean ridge into segments of variable lengths (tens to hundreds of kilometres). Independent of length, most ridge segments have arched along-strike topographic profiles—i.e., a depth minimum is located approximately midway along the ridge segment, and depths increase toward the ends of the segment (Fig. 3B). Each ridge segment is characterized by its own distinctive along-strike profile in terms of relief and gradient from central high to segment ends, and depth of the central high. The extent to which axial depths increase from central high to segment ends ranges from tens to thousands of metres; the largest changes in relief are associated with ridge segments along more slowly accreting ridges (e.g., Mid-Atlantic Ridge). At fast-spreading ridges, which usually exhibit axial highs, the axial high increases steadily in cross-section area with increasing proximity to the elevated mid-sections of individual segments (Macdonald and Fox, 1988; Scheirer and Macdonald, 1993).

The scale of ridge segmentation discussed above is relatively easy to recognize because the ridge axis is clearly offset along strike. Recent high-resolution imaging and sampling of the ridge axis in some areas has defined morphologic, bathymetric, and geochemical changes along strike that suggest a finer, fourth-order scale of segmentation that is superimposed on the tens to hundreds of kilometres-long segmentation discussed above (Fig. 2) (e.g., Langmuir et al., 1986). The along-strike arch-shaped architecture is retained at this small scale, but the wavelength is on the order of kilometres, and the relief is low. Individual fault traces and volcanic structures along the axis commonly reflect these deviations in axial linearity by exhibiting right- or left-stepping (<1 km) en echelon patterns.

A host of geologic observations, including the regular undulation of the crest of the ridge, which correlates with its cross-section area (Scheirer and Macdonald, 1993), seismic evidence for an axial melt reservoir (e.g., Detrick et al., 1987; Vera et al., 1990; Harding et al., 1993; Toomey et al., 1990), geochemical anomalies, and the locations of discontinuities has led to the development of a magma supply model for ridge segmentation. In the magma supply model, the generation, transport, and distribution of melt from the upper mantle is enhanced beneath the shallow, swollen region of each segment and is depleted at the ends of each segment near overlapping spreading centers and other discontinuities (see Macdonald et al., [1991], Langmuir et al. [1986], Sinton and Detrick [1992], and Solomon and Toomey [1992] for reviews). As the plates spread apart, partial melting of mantle rocks occurs due to adiabatic decompression at depths of 30 to 60 km. The buoyant melt segregates from residual solid mantle and ascends to fill shallow magma chambers within the crust along the ridge axis. These melts locally swell the crustal magma reservoirs, and buoyant forces associated with the melt and a surrounding halo of hot, melt-impregnated low-density rock create a local shoaling of the ridge crest. Continuous injection of melt leads to local eruptions, migration of magma away from the locus of upwelling, and expansion of the axial magma chamber along strike. The laterally migrating magma loses hydraulic head with increasing distance from the center of magma replenishment; as a result, the depth of the ridge axis steadily increases along strike. As magma migrates

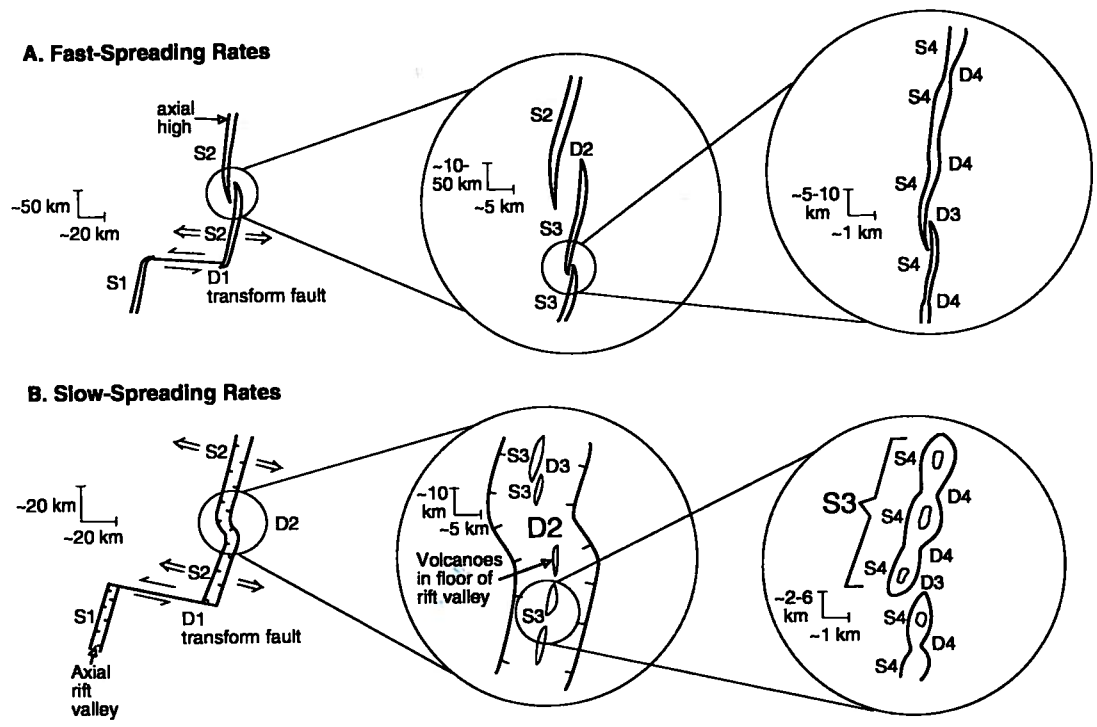

Figure 2. A proposed hierarchy of ridge-axis discontinuities of orders 1 through 4 for slow (bottom) and fast (top) spreading centers (after Macdonald et al., 1991). S1, 2, 3, 4 are ridge segments of order 1, 2, 3, 4, and D1, 2, 3, 4 are ridge-axis discontinuities of order 1, 2, 3, 4. Thus, a segment is first-order if it is bounded at both ends by first-order discontinuities, and second-, third-, or fourth-order if it is bounded at one (or both) end(s) by second-, third-, or fourth-order discontinuities. At both fast- and slow-spreading centers, first-order discontinuities are transform faults. Examples of second-order discontinuities are overlapping spreading centers on fast-spreading ridges and oblique shear zones on slow-spreading ridges. Third-order discontinuities are small overlapping spreading centers on fast-spreading ridges and intervolcano gaps on slow-spreading ridges. Fourth-order discontinuities are deviations from axial linearity (devals) resulting in slight bends or lateral offsets of the axis of less than 1 km on fast-spreading ridges and are intravolcano gaps on slow-spreading ridges. This four-tiered hierarchy of segmentation may really be a continuum. It has been established, for example, that fourth-order segments and discontinuities can grow to become third-, second-, and even first-order discontinuities and vice versa at both slow- and fast-spreading centers. Intermediate-rate spreading centers (40–90 mm/yr) tend to have the characteristics of slow-spreading segments and discontinuities when they are magmatically starved, and those of fast-spreading centers when magmatically robust. Even a fast-spreading center can have slow-spreading characteristics temporarily during periods of magma drought .

TABLE 1. CHARACTERISTICS OF RIDGE SEGMENTATION

	Order 1	Order 2	Order 3	Order 4
Segments				
Length (km)*	600 ±300 (400 ±200)	140 ±90 (50 ±30)	50 ±30 (15 ±10?)	14 ±8 (7 ±5?)
Longevity (yr)	>5 x 10^6	0.5–5 x 10^6 (0.5–10 x 10^6)	~10^4 – 10^5 (?)	~10^2 – 10^4 (?)
Discontinuities				
Offset (km)	>30	2–30	0.5–2.0	<1
Age (yr)†	>0.5 x 10^6 (>2 x 10^6)	<0.5 x 10^6 (<2 x 10^6)	~0	~0
Off-axis trace	Fracture zone	V-shaped discordant zone	None	None

Note: After Macdonald et al. (1991). Information for fast-spreading (>60 mm/yr) ridges, if it differs from that for slow-spreading ridges, is in parentheses.

*Errors are ±1σ.

†Of seafloor that is juxtaposed to the spreading axis at a discontinuity.

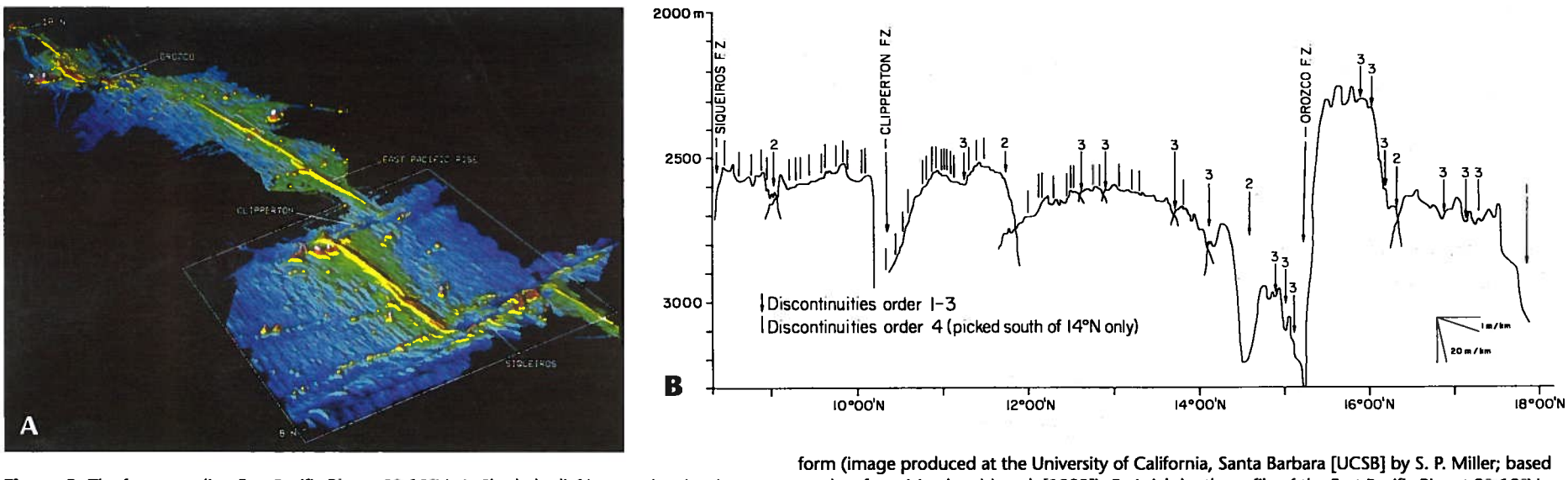

Figure 3. The fast-spreading East Pacific Rise at 8°–18°N. A: Shaded relief image; the view is toward the northeast. The white boxes show the locations of images in Figure 4 (foreground) and Figure 7 (see Fig. 4 for color depth scale). The image is of an area 1100 km long and about 350 km wide. The East Pacific Rise is the elevated north-south–trending region in the red-yellow depth range. The Siqueiros transform (foreground) is followed by the 9°N overlapping spreading centers, the Clipperton transform, the 11°45'N overlapping spreading center, and the Orozco transform (image produced at the University of California, Santa Barbara [UCSB] by S. P. Miller; based on data from Macdonald et al. [1993]). B: Axial depth profile of the East Pacific Rise at 8°–18°N taken from Macdonald et al. (1993). The numbers correspond to ridge axis discontinuities of orders 1 through 3. Fourth-order discontinuities (unlabeled vertical lines) are identified only south of 14°N, so the lack of fourth-order discontinuities north of 14°N indicates only that they have not been identified yet. In contrast to discontinuities of orders 1–3, fourth-order discontinuities have little or no axial depth anomaly.

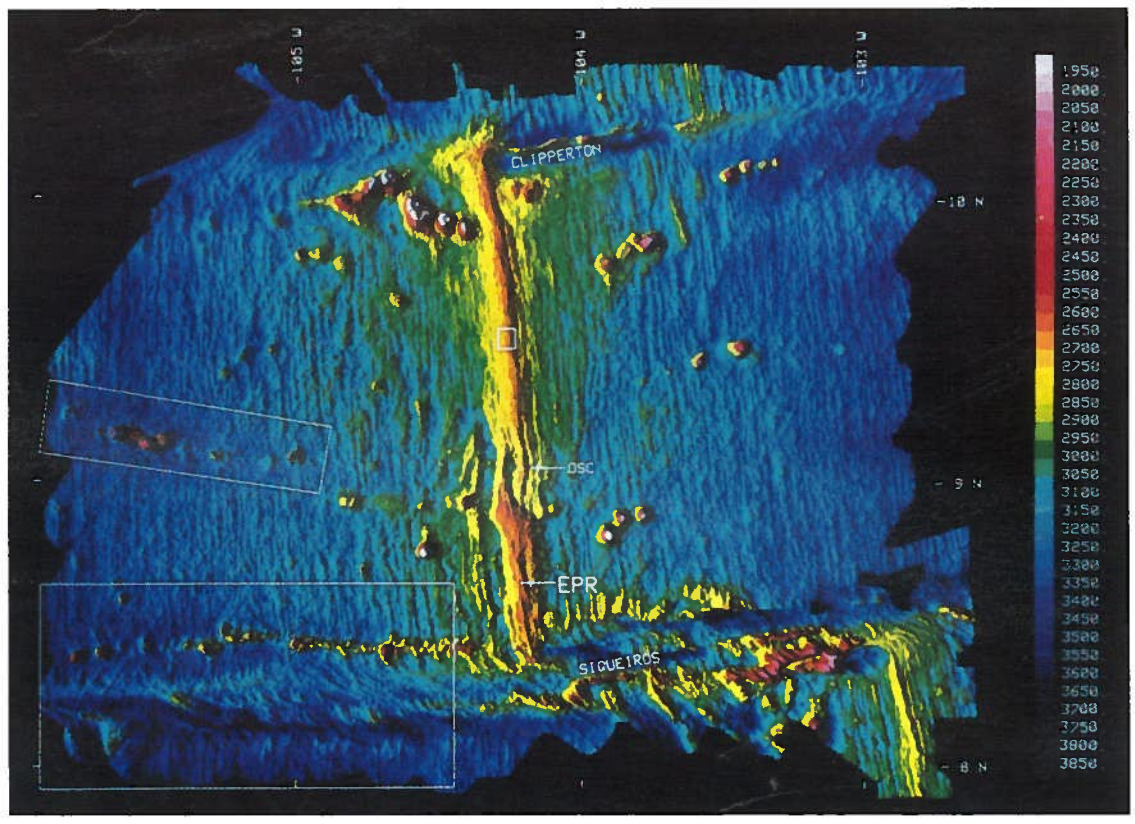

Figure 4. Sea Beam and SeaMARC II bathymetry merged in the Office of Naval Research East Pacific Rise Natural Laboratory (image produced at UCSB by S. P. Miller; based on data from Macdonald et al. [1993]). Subtle northeast-southwest grain is an artifact of SeaMARC II bathymetry parallel to the ship track. EPR is East Pacific Rise; OSC is 9°N overlapping spreading centers. Boxes show locations of side-scan sonar images of Figures 6A, 6B and 6C. There are no clear vestiges of the 300–400-m-high axial region of the East Pacific Rise on the rise flanks; as it cools, the shallow elevation disappears. Lineated north-south relief on the flank is produced by normal faulting (dip toward and away from the axis) and minor volcanism. On the ridge flanks adjacent to the 9°N overlapping spreading center, a V-shaped discordant zone indicates southward migration of the discontinuity at 52 mm/yr within the past ~1.0 m.y. The west-flank discordant zone comprises abandoned curvilinear ridge tips that reflect episodic clipping of the western ridge tip at the overlapping spreading center. The east-flank discordant zone consists of greater depths. Southward migration of the discontinuity has not been steady but has involved a series of episodic and dueling propagation events with rates ranging from <10 mm/yr to >500 mm/yr.

at depth along the ridge, continued extension fractures the overlying brittle carapace of frozen lava. Magmas then use these fractures as conduits to the seafloor, and volcanic eruptions follow the advancing crack front. The process outlined above occurs repeatedly as plate separation continues. In this magmatic model for a spreading center, ridge-axis discontinuities occur at the distal ends of magmatic pulses and define the ends of ridge segments (Figs. 3, 5A).

At slow-spreading ridges, seismic studies have not revealed a magma reservoir (Detrick et al., 1990). However, a similar pattern of segmented upwelling may still occur there, and very small pockets of melt or highly episodic magma chambers may be present (Smith and Cann, 1990). Large, bulls-eye–shaped gravity anomalies occur over ridge segments defined by second-order discontinuities on the Mid-Atlantic Ridge (Lin et al., 1990; Kuo and Forsyth, 1988; Blackman and Forsyth, 1991). Corrected to remove the gravitational effects of topography, these anomalies indicate that low-density upper mantle or thickened oceanic crust is present beneath the midsections of segments. Kuo and Forsyth (1988) proposed that these anomalies are best explained by a three-dimensional pattern of upwelling hot mantle material. The pattern of mantle upwelling may become less three-dimensional (Lin and Phipps Morgan, 1992), and magma migration within axial magma reservoirs may be more efficient at higher spreading rates (J. R. Cochran et al., unpublished).

Editor's Note: This is the first part of a two-part article. ■

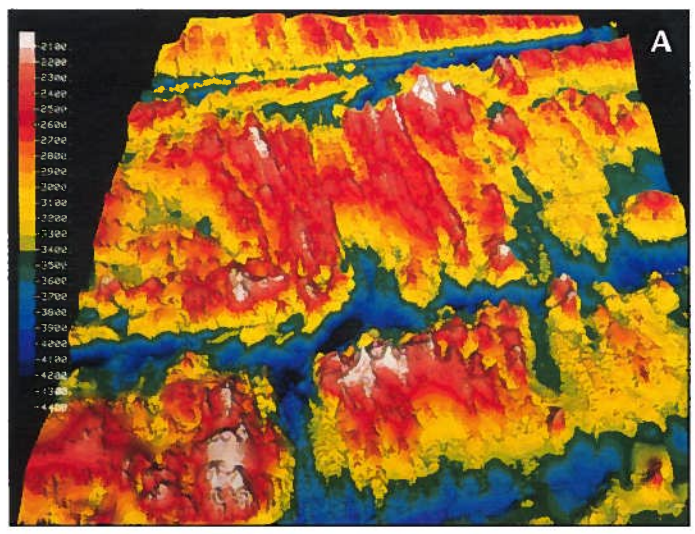

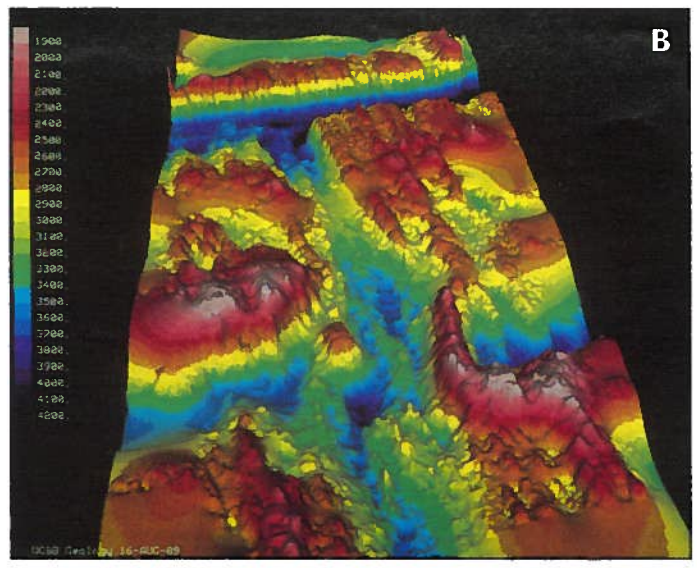

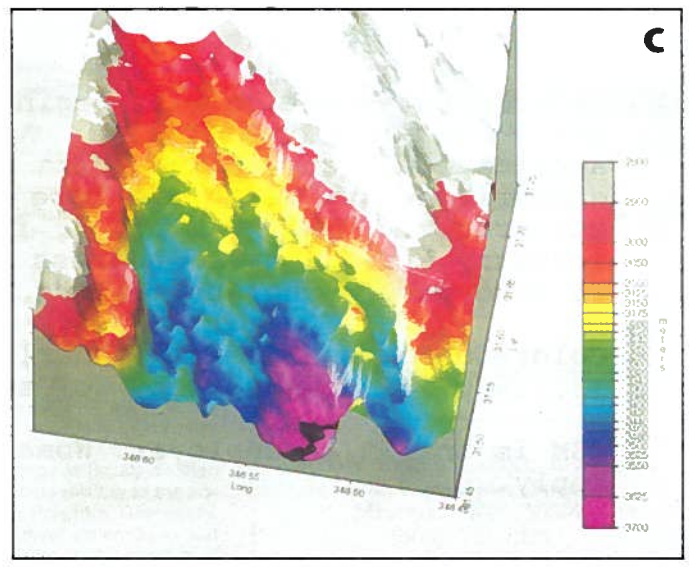

Figure 5. A: A shaded relief image of slow-spreading southern Mid-Atlantic Ridge (31°–34°S) looking northeast. The Meteor transform is in the foreground, then the 33°30'S second-order discontinuity; the Cox transform is in the background. An axial rift valley marks the spreading axis; it shoals to 200 m deep along 20% of the length of the segment shown but does not disappear. (Produced at UCSB by Charles Weiland, using data from Fox et al. [1991].) B: A shaded relief image with the Cox transform in the background and the 31°20'S second-order discontinuity in the foreground (a 12 km right-lateral jog of the axial rift valley). The view is toward the south. (Produced at UCSB by Suzanne Carbotte, using data from Grindlay et al. [1991].) C: Blow-up map of the neovolcanic zone within the axial rift valley from B (10 m contour interval). Note the many small conical volcanoes similar to those observed in the North Atlantic (Smith and Cann, 1990). (Produced at UCSB by Charles Weiland, using data from Fox et al. [1991].)